ON-LINE DETECTION AND ESTIMATION OF GASEOUS POINT SOURCES USING SENSOR NETWORKS

S. Agostinho, J. Gomes

Institute for Systems and Robotics – Instituto Superior Técnico, University of Lisbon, Portugal

`sergio.agostinho@tecnico.ulisboa.pt, jpg@isr.ist.utl.pt`

ABSTRACT

The current work tackles the detection and localization of a diffusive point source, based on spatially distributed concentration measurements acquired through a sensor network. A model-based strategy is used, where the concentration field is modeled as a diffusive and advective-diffusive semi-infinite environment. We rely on hypothesis testing for source detection and maximum likelihood estimation for inference of the unknown parameters, providing Cramér-Rao Lower Bounds as benchmark. The (non-convex and multimodal) likelihood function is maximized through a Newton-Conjugate Gradient method, with an applied convex relaxation under steady-state assumptions to provide a suitable source position initialization. Detection is carried out resorting to a Generalized Likelihood Ratio Test. The framework's robustness is validated against a numerically simulated environment generated by the Toolbox of Level Set Methods, which provides data (loosely) consistent with the model.

Index Terms— Diffusive Source Localization, Maximum Likelihood Estimator, Newton-Conjugate Gradient, Generalized Likelihood Ratio Test, Sensor Network

1. INTRODUCTION

The subject of diffusive source localization, or more generally, diffusive phenomena parameter estimation, has been mostly covered during the last decade. Focusing on methods that allow detection and estimation of a continuous source location in a diffusive and advective environment, the two most common approaches are estimation resorting to a Maximum Likelihood Estimator (MLE) or an Extended Kalman Filter (EKF). The MLE provides modeling flexibility which potentially enables more complex scenarios to be tackled, but requires an analytical solution to the governing Partial Differential Equation (PDE) that may be difficult to determine and a generally non-linear optimization problem [1]. The EKF approach requires a linear approximation with respect to the variables of interest followed by discretization for its state-space formulation, which can be challenging to derive in closed form [2]. In a conceptually different approach, Lu et al. [3] showed that the diffusive field generated by an impulsive point source is described, at different points in space, by scaled and shifted replicas of a single prototype

function, whose properties enable the source parameters to be determined through a set of linear equations.

In our work, source detection and localization is achieved through the implementation of a detection and estimation framework, relying on data gathered by a Sensor Network (SN). Although the approach is generally based on [1], in this paper we actually cover all the required aspects to make the framework operational and contribute with a new method to address the (crucial) initialization of the optimization problem. The framework is governed by two distinct phases or operation modes. In the first phase, the source is assumed to start at an inactive state and the main focus is to accurately detect its transition to an active state. The detector requires estimates under both absent and active source hypotheses and the former are continuously refined until detection triggers. In the second phase, after the source has been detected, all the newly gathered data is used to refine the parameters' estimates under the active source hypothesis. [4]

The rest of the paper is organized as follows: Section 2 introduces the governing equations for diffusive and advective-diffusive environments; Section 3 presents the MLE based estimator and Cramér-Rao Lower Bounds (CRLBs); Section 4 covers the optimization problem and the convex relaxation approach used for initialization; Section 5 is dedicated to detection resorting to a Generalized Likelihood Ratio Test (GLRT); Section 6 illustrates the framework's performance in simulation and sensitivity to parameters' variation are tested; Section 7 sums up the work developed.

2. PHYSICAL MODELING

The environmental model is constrained by the following assumptions: a single fixed point source is considered, with known vertical coordinate (at ground level), that upon activation will release mass continuously at a constant rate; the medium is semi-infinite over a flat horizontal surface boundary (the floor), devoid of any physical obstacles; it has an unknown constant diffusion coefficient, which incorporates the contributions from both molecular and turbulent diffusion, as discussed in [1]; the wind flow is uniform and known (externally measured); buoyancy and gravity effects are negligible; the substance of interest is immune to chemical and other physical transformation processes; all sensors' positions are known and sampling occurs synchronously, with positions and timestamps assumed to be error free.

2.1. Diffusive Model

Let $\vec{r} = [r_x, r_y, r_z]^T$ denote s position vector in a three dimensional frame of reference and $c(\vec{r}, t)$ designate a given substance's concentration, as a function of space and time, and k to refer to the diffusion coefficient. From Fick's law of diffusivity and the continuity equation

$$\frac{\partial c(\vec{r}, t)}{\partial t} = k \nabla^2 c(\vec{r}, t). \tag{1}$$

Assuming a single point source that activates at t_0 [s] and starts releasing mass at a constant rate μ [Kg/s], placed at the boundary of a semi-infinite medium, such that $r_z = 0$ [m], leads to a slight modification to the solution presented in [1].

$$c(\vec{r}, t) = \frac{\mu}{2\pi k |\vec{r} - \vec{r}_s|} \text{erfc}\left(\frac{|\vec{r} - \vec{r}_s|}{2\sqrt{k(t - t_0)}}\right). \tag{2}$$

The source position, denoted by $\vec{r}_s$, and its mirror image overlap. The function erfc stands for the complementary error function, defined as $\text{erfc}(g) = \frac{2}{\sqrt{\pi}} \int_g^\infty \exp\left(-h^2\right) \, dh$.

2.2. Advective-Diffusive Model

When the influence of wind is considered, another term must be added to (1)

$$\frac{\partial c(\vec{r}, t)}{\partial t} = k \nabla^2 c(\vec{r}, t) - \nabla \cdot (c(\vec{r}, t) \vec{v}). \tag{3}$$

Considering the stated assumptions, now incorporating the uniform wind flow, yields an expression similar to the one derived in [1], once more exploiting the fact that the source and its mirror image positions are equal

$$
\begin{aligned}
c(\vec{r}, t) = \; & \frac{\mu}{4\pi k |\vec{r} - \vec{r}_s|} \exp\left(\frac{(\vec{r} - \vec{r}_s) \cdot \vec{v}}{2k}\right) \\
& \times \left[\exp\left(\frac{|\vec{r} - \vec{r}_s||\vec{v}|}{2k}\right) \right. \\
& \times \text{erfc}\left(\frac{|\vec{r} - \vec{r}_s|}{2\sqrt{k(t - t_0)}} + |\vec{v}|\sqrt{\frac{t - t_0}{4k}}\right) \\
& + \exp\left(-\frac{|\vec{r} - \vec{r}_s||\vec{v}|}{2k}\right) \\
& \left. \times \text{erfc}\left(\frac{|\vec{r} - \vec{r}_s|}{2\sqrt{k(t - t_0)}} - |\vec{v}|\sqrt{\frac{t - t_0}{4k}}\right) \right]
\end{aligned} \tag{4}
$$

2.3. Measurement Model

The SN considered is composed of multiple individual chemical sensors, capable of measuring point concentrations at their placed location. The measurement model used was the one proposed in [1].

$$y(\vec{r}, t) = c(\vec{r}, t) + b + e(\vec{r}, t). \tag{5}$$

Equation (5) comprises following terms: $y(\vec{r}, t)$ is the measured value reported by the sensor; $c(\vec{r}, t)$ is the concentration of the substance of interest present at the sensor; b is the sensor bias, considered to be spatially uniform and time invariant, included as a way to represent the sensors' sensitivity to undesirable substances; $e(\vec{r}, t)$ represents zero mean white Gaussian measurement noise, with unknown variance σ_e^2, independent between sensors.

3. PARAMETER ESTIMATION

From the models governing the physical phenomena of interest, the lumped parameter vector comprises $[r_{s_x}, r_{s_y}, k, t_0, \mu, b, \sigma_e^2]^T$ with: r_{s_x} and r_{s_y} as the source's horizontal coordinates; k as the total diffusivity coefficient; t_0 as the activation instant; μ as the source release rate; b as the sensor bias; σ_e^2 the noise variance.

3.1. Maximum Likelihood Estimator

Recall (5) and consider m sensors, whose locations are all known, that perform n measurements: $y(\vec{r}_i, t_j)$, $1 \leq i \leq m$, $1 \leq j \leq n$. $\mathbf{y}$ will be a (mn)-dimensional vector whose $(m(j-1) + i)$th component will be $y(\vec{r}_i, t_j)$. Extend the same reasoning to the noise vector $\mathbf{e}$. As highlighted in [1], at least three sensors and samples acquired at two different instants are required to determine the source location. Rearranging the parameter vector as $[\theta^T, \mathbf{x}^T, \sigma_e^2]^T$, where $\mathbf{x} = [\mu, b]^T$ and $\theta = [r_{s_x}, r_{s_y}, k, t_0]^T$, we can write

$$\mathbf{y} = \mathbf{A}(\theta)\mathbf{x} + \mathbf{e}, \tag{6}$$

$$\mathbf{A}(\theta) = [\mathbf{a}(\theta) \quad \mathbb{1}]. \tag{7}$$

The spatial and temporal dependence are omitted to streamline the notation. In (7), each element of $\mathbf{a}(\theta)$, $a_{ij}(\theta) = c(\vec{r}_i, t_j, \theta)/\mu$. The symbol $\mathbb{1}$ denotes a (mn)-dimensional vector of 1's. The maximum likelihood estimates can be determined through [1]

$$\hat{\theta} = \arg \max_\theta \left\{ \mathbf{y}^T \mathbf{P_A}(\theta) \mathbf{y} \right\}, \tag{8}$$

$$\hat{\mathbf{x}} = \left[\mathbf{A}^T(\hat{\theta}) \mathbf{A}(\hat{\theta}) \right]^{-1} \mathbf{A}^T(\hat{\theta}) \mathbf{y}, \tag{9}$$

$$\hat{\sigma}_e^2 = (mn)^{-1} \mathbf{y}^T \mathbf{P_A^\perp}(\hat{\theta}) \mathbf{y}. \tag{10}$$

where $\mathbf{P_A}(\theta)$ and $\mathbf{P_A^\perp}(\theta)$ stand for the projection matrix and the complementary projection matrix on the column space of $\mathbf{A}(\theta)$, respectively.

$$\mathbf{P_A}(\theta) = \mathbf{A}(\theta)[\mathbf{A}^T(\theta)\mathbf{A}(\theta)]^{-1}\mathbf{A}^T(\theta), \tag{11}$$

$$\mathbf{P_A^\perp}(\theta) = \mathbf{I} - \mathbf{P_A}(\theta), \tag{12}$$

where $\mathbf{I}$ denotes the identity matrix. As shown in [1] the Maximum Likelihood (ML) estimate for the vector of nonlinear parameters, θ, is equivalently given by

$$\hat{\theta} = \arg \max_\theta \mathcal{L}(\theta),$$

$$\mathcal{L}(\theta) = \frac{[(\mathbf{y}^T \mathbf{a}(\theta)) - (mn)^{-1}(\mathbb{1}^T \mathbf{y})(\mathbb{1}^T \mathbf{a}(\theta))]^2}{(\mathbf{a}^T(\theta)\mathbf{a}(\theta)) - (mn)^{-1}(\mathbb{1}^T \mathbf{a}(\theta))^2}. \tag{13}$$

(a) Source r_{s_x} coordinate

(b) Source r_{s_y} coordinate

(c) Diffusivity k
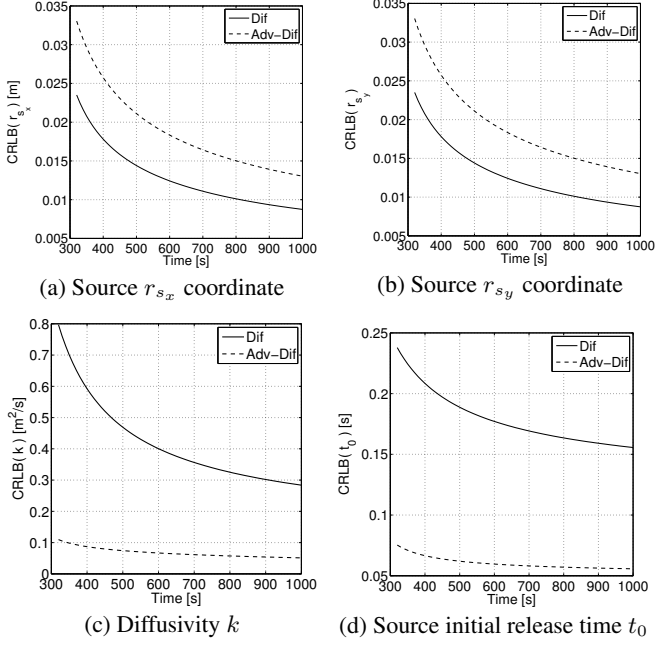
(d) Source initial release time t_0

Fig. 1: Cramér-Rao lower bounds (square root) for θ under a diffusive (solid line) and an advective-diffusive (dashed line) environment.

3.2. Cramér–Rao Lower Bound

The CRLBs derived in [1] are given by

$$\text{CRLB}(\theta) = \frac{\sigma_e^2}{\mu^2}\{\mathbf{D}^T(\theta)\mathbf{P}_\mathbf{A}^\perp(\theta)\mathbf{D}(\theta)\}^{-1}, \quad (14)$$

$$\text{CRLB}(x) = \sigma_e^2\{\mathbf{A}^T(\theta)\mathbf{P}_\mathbf{D}^\perp(\theta)\mathbf{A}(\theta)\}^{-1}, \quad (15)$$

$$\text{CRLB}(\sigma_e^2) = \frac{2\sigma_e^4}{mn}, \quad (16)$$

with $(mn \times 4)$ dimensional matrix $\mathbf{D} = \frac{\partial \mathbf{a}(\theta)}{\partial \theta}$. A simulation was composed to display the lower bounds. The conditions were: 1000 [s] simulation duration, in either a diffusive and an advective-diffusive environment, with $k = 25$ [m^2/s] and $\vec{v} = [1,1,0]^T$ [m/s]; source placed at $\vec{r_s} = [45,45,0]^T$ [m], that initiates its release at $t_0 = 200$ [s], at a constant rate of $\mu = 1$ [Kg/s]; nine sensors placed on a uniform grid at $r_{x_i} \in \{25,50,75\}$ [m], $r_{y_i} \in \{25,50,75\}$ [m] and $r_{z_i} = 0$ [m], subject to a bias of $b = 1 \times 10^{-4}$ [Kg/m^3] and Gaussian noise error with standard deviation $\sigma_e = 2 \times 10^{-6}$. The sampling interval is $\Delta t = 10$ [s]. Figure 1 shows the evolution of the CRLBs. The values shown are the square roots of the computed bounds. The bounds are lower for the source location parameters in the pure diffusive case and lower for the remaining parameters in the advective-diffusive case. Therefore, it should result in potentially better estimates for the source location under pure diffusive conditions and better estimates for the remaining parameters under advective-diffusive conditions. These bounds were achieved over an average Signal-to-Noise Ratio (SNR) of $\text{SNR}_D = 44.46$ [dB] and $\text{SNR}_{AD} = 44.05$ [dB] for the diffusive and advective-diffusive cases, respectively.

4. LIKELIHOOD FUNCTION MAXIMIZATION

In this section we describe our iterative approach for maximizing the likelihood function, as well as the crucial initialization procedure. The former topic was covered only superficially in [1], whereas the latter is very different from what was proposed in that work. The function $\mathscr{L}(\theta)$ is multimodal, requiring good-quality initialization to reach a suitable maximum (hopefully a global one). The feasible set is bounded by $k > 0$ and $t - t_0 > 0$, since the diffusivity loses its physical meaning if the value is nonpositive, and (2), (4) are not valid prior to source activation. As commonly done in the literature, maximization of $\mathscr{L}(\theta)$ is converted into minimization of $f(\theta) = -\mathscr{L}(\theta)$. An iterative line search strategy using the Armijo backtracking for step control [5] is used. At iteration κ, with parameter vector θ^κ and descent direction d^κ, the step β is chosen such that

$$f(\theta^\kappa + \beta\, d^\kappa) \leq f(\theta^\kappa) + \delta\,\beta\nabla f(\theta^\kappa)^T d^\kappa. \quad (17)$$

The δ term is a constant that allows to further specify the rate of descent. Backtracking was exploited to ensure that iterates always remain in the feasible set for k and t_0. The step is initialized with $\beta = 1$ as is common when in Newton or Quasi-Newton methods. The descent direction d^κ is chosen through a Newton-Conjugate Gradient (CG) method [5] solving

$$\underset{d^\kappa}{\text{minimize}} \quad \|r^\kappa\| \quad (18)$$

$$\text{subject to} \quad r^\kappa = \nabla^2 f(\theta^\kappa)d^\kappa + \nabla f(\theta^\kappa) \quad (19)$$

$$\|r^\kappa\| \leq \eta^\kappa\|\nabla f(\theta^\kappa)\|^\varrho. \quad (20)$$

Whenever possible, $\varrho = 2$ in (20) ensures quadratic convergence .

4.1. Initialization

Good-quality initialization of the iterative likelihood maximization algorithm is required to obtain desirable estimates of the source parameters. The proposed initialization method exploits the link between a stationary diffusive field and the propagation model used for localization of radio sources based on received power [6, 7], capitalizing on known accurate and convex (hence globally convergent) formulations for the latter problem. Despite the stationary assumption, in practice the method provides sufficiently accurate estimates of the source position when fed non-steady state concentrations, as demonstrated by our numerical results. Assuming a solely diffusive case and that enough time has passed to achieve a stationary regime, (2), (5)

$$y(\vec{r_i}, \infty) = \frac{\mu}{2\pi k\|\vec{r_i} - \vec{r_s}\|} + b + e. \quad (21)$$

The parameter $\vec{r_i}$ is only two dimensional in this case. Squaring both left and right sides of the equations and lumping together all cross multiplicative and second order terms involving the bias and Gaussian error into a new error term denoted by ε,

$$c_i = \frac{c_s}{\|\vec{r_i} - \vec{r_s}\|^2} + \varepsilon, \quad (22)$$

where $c_i = y(\vec{r_i}, \infty)^2$ and $c_s = (\mu/2\pi k)^2$. Adopting a Least Squares estimator

$$\hat{\vec{r_s}} = \arg\min_{\vec{r_s}, c_s} \sum_i \left(c_i \|\vec{r_s} - \vec{r_i}\|^2 - c_s\right)^2. \qquad (23)$$

The term c_s is treated as an additional optimization variable allowing it to absorb modelling differences from using (21) in a non stationary situation and from neglecting the bias term. It also avoids the need for knowing μ and k in advance. Similarly to the procedure performed in [6], it is reasonable to assume that with small enough residual error the l_2 norm minimized on (23) can be approximated by the l_1 norm leading to

$$\hat{\vec{r_s}} = \arg\min_{\vec{r_s}, c_s} \sum_i \left|c_i \|\vec{r_s} - \vec{r_i}\|^2 - c_s\right|. \qquad (24)$$

Defining the auxiliary variable z such that

$$\|\vec{r_s} - \vec{r_i}\|^2 = z - 2\vec{r_s}^T \vec{r_i} + \vec{r_i}^T \vec{r_i}, \qquad (25)$$
$$z = \vec{r_s}^T \vec{r_s}, \qquad (26)$$

we can relax (24) as a semidefinite program

$$\underset{\vec{r_s}, c_s, h_i, z}{\text{minimize}} \quad \sum_i h_i \qquad (27)$$

$$\text{subject to} \quad -h_i \leq c_i(z - 2\vec{r_s}^T \vec{r_i} + \vec{r_i}^T \vec{r_i}) - c_s \leq h_i \qquad (28)$$

$$z \geq \vec{r_s}^T \vec{r_s}, \qquad (29)$$

solved resorting to available general-purpose convex solvers. Even thought $\vec{r_s}$ and c_s are both obtained from (27)-(29), we found that only the former has enough quality to initialize the Newton-CG method. Attempts to extract k from c_s proved to be unreliable due to the approximation errors introduced. The most significant ones are: $t \ll \infty$ thus erfc $\neq 1$; the bias term being inadequately neglected. In the context of initialization the advective-diffusive case is treated as solely diffusive and initialized similarly, exploiting the idea that the modelling differences should not be significant enough to corrupt the estimates up to a certain wind speed. The diffusivity and initial release time parameters were coarsely initialized: the former through the use of a constant value $k = 10$, close to the ones used in [1]; the latter was initialized as $t_0 = t_1 - \Delta t$, where Δt is the sample time, relying on an assumption of a higher probability of source activation moments prior to the earliest timestamp of the measurements included in the likelihood function.

5. DETECTION

Detection enables the differentiation between the inactive and active states of the source and defines when the shift in the framework's operating mode occurs. The case at hand is one of a binary hypothesis. Consider $\mathcal{H}_0$ as the null hypothesis or absent source, and $\mathcal{H}_1$ as the alternate hypothesis or active source. The lack of prior probabilities for both hypothesis, $p(\mathcal{H}_0)$ and $p(\mathcal{H}_1)$, precludes a Bayesian formulation. We

adopted the Neyman Pearson approach with the intent of maximizing the probability of detection P_D for a given probability of false-alarm P_{FA}. Both the signal and noise probability density functions have unknown parameters. The Generalized Likelihood Ratio Test (GLRT) is commonly used to tackle parametric detection problems such as this one, and usually performs well. The statistical test is given by
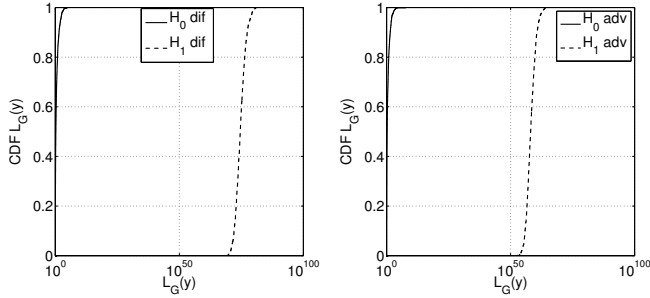
$$L_G(\mathbf{y}) = \frac{p(\mathbf{y}; \hat{\phi}_1, \mathcal{H}_1)}{p(\mathbf{y}; \hat{\phi}_0, \mathcal{H}_0)} \underset{\mathcal{H}_0}{\overset{\mathcal{H}_1}{\gtrless}} \gamma, \qquad (30)$$

where $\hat{\phi}_1 = [r_{s_x}, r_{s_y}, k, t_0, \mu, b_1, \sigma_{e_1}^2]^T$ and $\hat{\phi}_0 = [b_0, \sigma_{e_0}^2]^T$ are determined by the MLE under $\mathcal{H}_1$ and $\mathcal{H}_0$, respectively. Since the MLEs under $\mathcal{H}_1$ and $\mathcal{H}_0$ do not yield the same results, a subscript is added to b and σ_e^2 to clarify the correspondent hypothesis. $\hat{\phi}_1$ is estimated through (8)-(10) and to determine $\hat{\phi}_0$ one must take into account that under $\mathcal{H}_0$, $P(y(\vec{r}, t)) = \mathcal{N}(b_0, \sigma_{e_0}^2)$, therefore $\hat{b}_0 = (mn)^{-1}\mathbf{y}^T\mathbb{1}$ and $\hat{\sigma}_{e_0}^2 = (mn)^{-1}(\mathbf{y} - \hat{b}_0\mathbb{1})^T(\mathbf{y} - \hat{b}_0\mathbb{1})$. Using all gathered observations indiscriminately can result in corrupt estimates under $\mathcal{H}_1$ since the estimator cannot cope with observations prior to the source activation, resulting in an incorrect bounding of the solution space along t_0. Given that the activation instant is not known, one is forced to make a guess. This situation was tackled employing RANdom SAmple Consensus (RANSAC) and selecting the best candidate for the activation instant. The best n_0 is the one for which the best correspondence is obtained between real and expected measurements at the sensors, based on the computed estimates. Having picked n_0, (30) assumes the form

$$L_G(\mathbf{y}_{n_0+1:n}) = \left(\frac{\hat{\sigma}_0^2}{\hat{\sigma}_1^2}\right)^{\frac{n-n_0}{2}} \exp\left(\frac{\|\mathbf{y}_{n_0+1:n} - \hat{b}_0\mathbb{1}\|^2}{2\hat{\sigma}_{e_0}^2}\right.$$
$$\left. - \frac{\|\mathbf{y}_{n_0+1:n} - (\mathbf{a}(\hat{\theta})\hat{\mu} + \hat{b}_1\mathbb{1})\|^2}{2\hat{\sigma}_{e_1}^2}\right). \qquad (31)$$

$$P_{FA} = \int_{\{\mathbf{y}: L_G(\mathbf{y}) > \gamma\}} p(\mathbf{y}; \mathcal{H}_0) \, d\mathbf{y} = \tau. \qquad (32)$$

The term γ is a threshold dependent on the false-alarm probability P_{FA}, given by (32). The non-linear dependence on $\mathbf{a}(\hat{\theta})$ and statistical dependence of $\hat{\theta}$ on $\mathbf{y}$ makes it difficult to determine the threshold in closed form; therefore, a Monte Carlo simulation was conducted to numerically estimate it, following the rule of thumb of $100/P_{FA}$ runs mentioned in [1]. An experiment was assembled for the simulation, defined in Section 3.2, allowing the following differences: under $\mathcal{H}_0$ the source is never active and under $\mathcal{H}_1$ the source activates at $t_0 = 0$ [s]. The collected measurements were taken at $\{10, 20, 30, 40\}$ [s]. The target was $P_{FA} = 0.01$ for a total amount of 10^4 runs. The empirical Cumulative Distribution Functions (CDFs) of the statistical test $\mathcal{L}_G(\mathbf{y}_{n_0+1:n})$ under both hypotheses are displayed in Figure 2. The values for $L_G(\mathbf{y}_{n_0+1:n})$ under advective condition are considerably lower in comparison with pure diffusive conditions. Despite being able to work with the entire set of observations, a moving window approach should be used, otherwise $L_G(\mathbf{y}_{n_0+1:n})$

(a) Test under solely diffusive conditions (b) Test under advective-diffusive conditions

Fig. 2: Empirical CDF of the statistical test (31), computed from multiple simulation runs. In half the simulations there was no source in the environment ($\mathcal{H}_0$) and in the remaining ones a source was present ($\mathcal{H}_1$). The detection threshold γ, chosen as a function of the false alarm probability P_{FA}, is picked from the obtained CDF.

can overflow due to the exponential dependence of $(\hat{\sigma}_0^2/\hat{\sigma}_1^2)$ on the window size. The number of required samples directly relates to the SNR inherent to the problem.

6. SIMULATION ENVIRONMENT, RESULTS AND DISCUSSION

The simulation environment was provided by the Toolbox of Level Set Methods (TLSM) for MATLAB, a toolbox developed to tackle time dependent Hamilton-Jacobi PDEs [8]. The TLSM uses Finite-Difference Methods (FDMs) on top of structured Cartesian grids to determine the evolution in time of the state vector. Albeit based on the same PDE and modelling similar transport mechanisms, the results from TLSM are computed resorting to approximations, contrary to the analytical closed-form expression used so far. The simulations tested consisted on: a total duration of 1000 [s]; an environment dictated by a diffusivity constant $k = 8.5$ [m^2/s] and uniform wind flow of $\hat{\nu} = [1, 1, 0]$ [m/s], in the advective case; a source placed at $\vec{r}_s = [35, 35, 0]$ [m] that initiates its release at $t_0 = 200$ [s], at a constant rate of $\mu = 1$ [Kg/s]; an uniformly spaced sensor grid of nine sensors placed at $r_{x_i} \in \{25, 50, 75\}$ [m], $r_{y_i} \in \{25, 50, 75\}$ [m] and $r_{z_i} = 0$ [m], subject to a bias of $b = 1 \times 10^{-4}$ [Kg/m^3] and Gaussian noise error with a standard deviation $\sigma = 2 \times 10^{-6}$ [Kg/m^3], making observations with a sampling time of $\Delta t = 10$ [s]. The results are displayed in Table 1. In general, the framework achieves good results in the task of detecting and localizing a diffusive point source. The TLSM generated field presents differences to the closed-form expressions, that are reflected on the accuracy of the estimates, making it extremely difficult for the CRLBs to be achieved. The source location parameters are the most resilient parameters to modelling errors. Detection occurs in the time instant following the source activation.

7. CONCLUSIONS

The current work extends on the approach taken by [1], presenting results for both the pure diffusive case and the

	Dif		Adv	
	$\lvert(\hat{x}-x)/x\rvert$	$\sqrt{\text{CRLB}(x)}$	$\lvert(\hat{x}-x)/x\rvert$	$\sqrt{\text{CRLB}(x)}$
$r_{s_x} = 35$ [m]	3.516E−03	2.635E−03	1.403E−02	5.509E−03
$r_{s_y} = 35$ [m]	3.573E−03	2.635E−03	1.386E−02	5.509E−03
$k = 8.5$ [m^2/s]	1.225E−01	2.460E−02	1.335E−01	1.922E−03
$t_0 = 200$ [s]	9.975E−04	4.971E−02	6.080E−03	4.848E−03
$\mu = 1$ [Kg/s]	1.472E−01	2.831E−03	3.479E−01	4.959E−04
$b = 1$E−04 [Kg/m^3]	1.700E−01	2.471E−07	1.495E−02	1.836E−07

Table 1: Simulation results, tested under the conditions mentioned in Section 6, using the TLSM to compute concentrations. Each line in the table corresponds to a parameter, where the real value is indicated in the leftmost column. For both diffusive and advective-diffusive conditions, we indicate the relative errors of the estimates and the squared root of the CRLBs.

advective-diffusive one. We address specific robustness and usability issues identified while trying to operationalize such approach, namely the challenging optimization problem inherent to the MLE where good initialization is fundamental and the observation selection strategy used in detection.

REFERENCES

[1] A. Nehorai, B. Porat, and E. Paldi, "Detection and localization of vapor-emitting sources," *IEEE Transactions on Signal Processing*, vol. 43, no. 1, pp. 243–253, Jan. 1995.

[2] E. Fox, J. Fisher, and A. Willsky, "Detection and localization of material releases with sparse sensor configurations," *IEEE Transactions on Signal Processing*, vol. 55, no. 5, pp. 1886 –1898, may 2007.

[3] Y. M. Lu, P. L. Dragotti, and M. Vetterli, "Localizing point sources in diffusion fields from spatiotemporal measurements," in *Proceeding of International Conference on Sampling Theory and Applications*, Singapure, may 2011.

[4] S. Agostinho, "Detection and localization of gaseous point sources for environmental assessment and monitoring of critical infrastructures using sensor networks," Master's thesis, Instituto Superior Técnico, june 2013.

[5] J. Nocedal and S. J. Wright, *Numerical Optimization*, ser. Springer Series in Operations Research. Springer, 1999.

[6] R. M. Vaghefi, M. R. Gholami, and E. G. Strom, "RSS-based sensor localization with unknown transmit power," in *IEEE International Conference on Acoustics, Speech and Signal Processing (ICASSP)*, 2011, pp. 2480–2483.

[7] S. Zejnilovic, J. Gomes, and B. Sinopoli, "Collaborative diffusive source localization in wireless sensor networks," in *Proceedings of the 20th European Signal Processing Conference (EUSIPCO)*, aug. 2012, pp. 704 – 708.

[8] I. M. Mitchell, "A toolbox of level set methods," University of British Columbia, Department of Computer Science, Tech. Rep. TR-2007-11, June 2007.